

# Synthesis of Graphite Nanosheets/Polyaniline Nanorods Composites with Ultrasonic and Conductivity

Zunli Mo, Huafeng Shi, Hong Chen, Guiping Niu, Zhongli Zhao, Yingbing Wu

Gansu Key Laboratory of Polymer Materials, College of Chemistry and Chemical Engineering, Northwest Normal University, Lanzhou 730070, China

Received 24 January 2008; accepted 27 September 2008

DOI 10.1002/app.29411

Published online 6 January 2009 in Wiley InterScience (www.interscience.wiley.com).

**ABSTRACT:** The graphite nanosheets/polyaniline (GN/PANI) nanorods composites were fabricated via ultrasonic polymerization of aniline monomer in the presence of GN, which was used as electric filling. The kind of doped acids, the concentration, and the contents of the GN were used as impact factors to the conductivity of the materials that were investigated. The structure of nanocomposites were characterized by FTIR and SEM. The results show that ultrasonic can effectively restrain the agglomerate of

the aniline and come to uniformity nanorods composites. The conductivity reached to 4.8 S/cm and 22 S/cm, respectively. The thermal stability of GN/PANI nanorods composites is superior to pure PANI as shown by TG analysis. © 2009 Wiley Periodicals, Inc. *J Appl Polym Sci* 112: 573–578, 2009

**Key words:** conducting polymers; nanocomposites; thermogravimetric analysis

## INTRODUCTION

Conductive polymers such as polyaniline (PANI), polypyrrole, and polythiophene are frequently used in the preparation of conductive composites. Among these polymers, PANI is often preferred because of the low cost of monomer, the reversible conductivity, the preparation with a high percent yield by oxidative polymerization, and its environmental stability.<sup>1,2</sup> However, ideal electroactive conducting polymers for direct use in electronic devices are not at present a reality because charge-carrier mobility is rather low. In the past decade, the intercalation of PANI into layered materials has received much attention because the confinement of PANI is expected to be highly ordered and to enhance charge-carrier mobility.<sup>3–6</sup> However, all these layered materials are electrical inhibitors that result in poor electrical conductivity. Polymer/graphite nanosheet (GN) composites have attracted much attention recently.<sup>7,8</sup> By blending polymer with expanded graphite (EG), one can achieve GN-reinforced polymer nanocomposites with electrical conducting per-

colation thresholds as low as 1.0–5.0 wt %, much lower than those filled with pristine graphite powder. Several GN composites such as PMMA/Ce(OH)<sub>3</sub>, Pr<sub>2</sub>O<sub>3</sub>/GN, GN/PPy, GN/AgCl/PPy have been prepared and investigated by Mo et al.'s group,<sup>9–11</sup> and PA6/GN,<sup>12</sup> PS/GN,<sup>13</sup> PMMA/GN,<sup>14</sup> UP/GN,<sup>15</sup> PANI/GN,<sup>16</sup> and poly(arylene disulfide)/GN<sup>17</sup> have been reported by other groups. These studies show that the high aspect ratio of the isolated GN makes them satisfy the percolation transition of conductivity at a remarkably low volume fraction in the polymer matrix. Nowadays, GN are the best filler for making conducting polymer/graphite nanocomposite.

Because GN were in nanoscale, they tended to accumulate each other and were difficult to be dispersed in PANI by traditional ways. Ultrasonic irradiation has been widely applied in chemical reaction and engineering. When an ultrasonic wave passes through a liquid medium, the effect of ultrasonic cavitation will take place and generate a very strong stirring environment. Therefore, ultrasound has been extensively used in dispersion, emulsifying, crushing, and activation of particles. In this case, ultrasonic was an effective way for the optimal dispersion of the GN in the PANI matrix, and it can effectively restrain the agglomerate of the aniline and come to uniformity of the nanorods composite. However, there is no report on GN/PANI nanorods composites via ultrasonic polymerization hitherto.

In this study, the GN/PANI nanorods composites were fabricated via ultrasonic polymerization of aniline monomer in the presence of GN, which was

Correspondence to: Z. Mo (mozl@163.com).

Contract grant sponsor: Natural Science Foundation of Gansu Province; contract grant number: 3ZS051-A25-050.

Contract grant sponsor: Science and Technology Tackle Key Problem Item of Gansu Province; contract grant number: 2GS064-A52-036-08.

Contract grant sponsor: Gansu Key Laboratory of Polymer Materials; contract grant number: ZD-04-14.

used as electric filling. Then, the kind of doped acids, the concentration, and the content of the GN as impact factors to the conductivity of the material were investigated.

## EXPERIMENTAL

### Materials

The graphite used in this study was expandable graphite, supplied from Shandong Qingdao Graphite Company (Qingdao, China). Aniline monomer and doubly distilled were purchased from Sinopharm Group Chemical Reagents Company (Shanghai, China) before use. The initiator, ammonium persulfate (APS) was bought from Xi'an Chemical Reagent Plant. *p*-Toluenesulfonic acid (TSA) and sulfuric ( $\text{H}_2\text{SO}_4$ ) were of analytical grade and used as received.

### Preparation of graphite nanosheets

GNs were prepared as proposed in Refs. 9–11. In our earlier work, the structure can also be seen. The expandable graphite was heat treated at  $950^\circ\text{C} \pm 10^\circ\text{C}$  for 15 s to obtain EG particles. The EG was immersed in 75% aqueous alcohol solution in an ultrasonic bath. The mixture was ultrasonic for 10 h, and then it was filtered and washed with enough distilled water and ethyl alcohol. The obtained graphite powers called GNs were dried under vacuum at ambient temperature for 12 h.

### Preparation of the graphite nanosheets/polyaniline nanorods composites

Aniline (2 mL) and 2.5 g of APS were dissolved in 50 mL acid solution ( $\text{H}_2\text{SO}_4$  or TSA) in two beakers, respectively. The concentrations of the acid solution we choosed were 0.1, 0.5, 1.0, 1.5, 2.0, 3.0, 4.0 mol/L. A certain amount of GNs were added to the acidic aniline solution. The mixture was ultrasonicated for 1 h to obtain uniform and steady state. The acidic solution of APS was added dropwise to the aniline-containing beaker to initiate the polymerization. After that, ultrasonication was continued for 6 h at  $30^\circ\text{C}$  to ensure the completion of polymerization. The green powder was collected on a Buchner funnel using a water aspirator, and the precipitate cake was filtered and washed exhaustively with deionized water until the filtrate became colorless. In every experiment, the concentration of the acid was identical. Finally, the cake was treated by placing in 2 mol/L acid solution with magnetic stirring for 3 h and then filtered and washed with deionized water for just one time to remove the excess acid. The nanocomposites were dried in vacuum ( $80^\circ\text{C}$ ) for 24 h and then powered in an agate mortar/pestle.

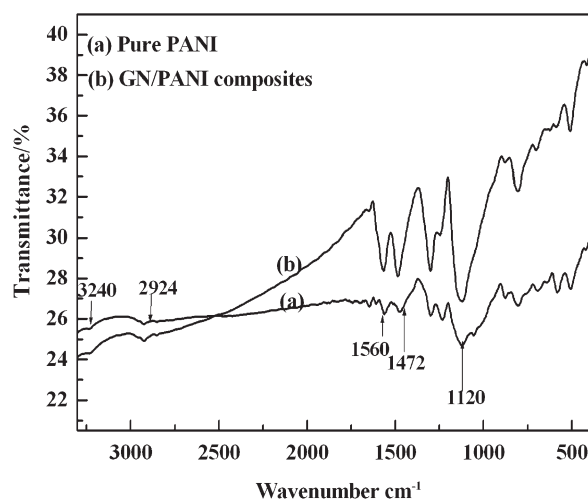


**Figure 1** FTIR spectra of (a) PANI and (b) NanoGs/PANI composites.

### Characterization and measurements

Scanning electron microscope (SEM; Hitachi, Japan, JEOL, JSM-6330F) was used to observe the morphologies of GN and GN/PANI nanorods composite. Before the examination, the specimens were coated with a thin layer of gold. Fourier-transform infrared spectra (FTIR) of the specimen in KBr pellets were recorded on an EQUINOX55 FTIR spectrometer (Bruker). The weight loss temperatures of the composites were determined with a Perkin-Elmer thermogravimetric analyzer (TG-DTA; model SSC-5200) from 20 to  $800^\circ\text{C}$  under environment atmosphere ( $10^\circ\text{C}/\text{min}$ ). The electrical conductivity measurements were made by the conventional four-point probe resistivity measurement system (Guangzhou, China, RTS-8) on pressed pellets of composite particles prepared at ambient temperature ( $25^\circ\text{C}$ ).

## RESULTS AND DISCUSSION

### IR spectroscopy studies

The FTIR spectra of PANI (a) and GN/PANI composites (b) are shown in Figure 1. The band at  $3240\text{ cm}^{-1}$  corresponds to N–H stretching of aromatic amine. To the left of the aromatic C–H stretching peak at  $2924\text{ cm}^{-1}$ , peak at  $1560\text{ cm}^{-1}$  is of quinine (Q) and  $1472\text{ cm}^{-1}$  for benzoide (B) ring deformation. The peak observed at  $1200$  and  $1400\text{ cm}^{-1}$  is a characteristic peak of intrinsic PANI indicating C–N stretching.

The main absorption peak for PANI is observed at  $1140\text{ cm}^{-1}$  and  $830\text{ cm}^{-1}$  because of the vibration mode of B–NH=Q or B–NH–B formed in doping reaction. All of these peaks are identical to those of PANI synthesized by a common method.<sup>18,19</sup> These evidences indicated that PANI was obtained by

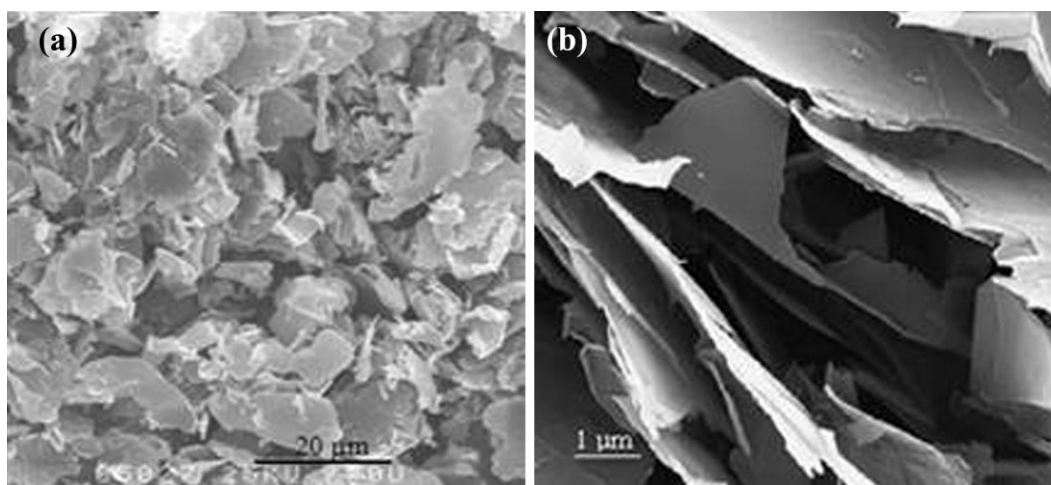


**Figure 2** SEM of GN: (a) lower magnification and (b) higher magnification.

ultrasonic polymerization of the ANI monomer. Meanwhile, compared with pure PANI, the characteristic peaks of the PANI molecules in the composites shifted to higher wavenumbers. The peak at  $1560\text{ cm}^{-1}$  is of quinine (Q) and  $1472\text{ cm}^{-1}$  for benzoide (B) ring deformation are shifted to  $1565$  and  $1484\text{ cm}^{-1}$ , respectively. This may be reasonably concluded that there was strong interaction between PANI and GNs. The addition of GNs probably resulted in the formation of hydrogen-bonding, which weakened the N–H as well as its stretching intensity. Moreover, GNs were, together with the results of SEM micrograph, dispersed in the PANI matrix.

### Morphology

We sonicated the EG in alcohol solution to gain shiny graphite powder. Figure 2 showed the SEM

image of sonicated EG. It revealed that the EG was tore to sheets with thickness of 30–80 nm and a diameter of 0.5–20 μm named GNs. The prepared GNs possessed a high aspect ratio (width-to-thickness) of around 100–500. The powder had an apparent density of  $0.015\text{ g/cm}^3$ , much smaller than that of the original flake graphite,  $2.25\text{ g/cm}^3$ . The result was similar to that reported by other researchers.<sup>20–22</sup> For example, Fukuda et al.<sup>23</sup> also treated EG with sonication and found that graphite sheets existed as separated nanosheets with the thickness of about 70 nm. It substantiated that the EG were composed of GNs. Such nanoscale dispersion facilitated the formation of the electrical conductive network in the polymer matrix at very low filler loading.

The typical SEM pictures of GN/PANI nanorods composites are presented in Figure 3. Figure 3(a,b) shows the samples magnified at  $2.0 \times 10^4$  times and  $3.0 \times 10^4$  times, respectively. We can clearly observe

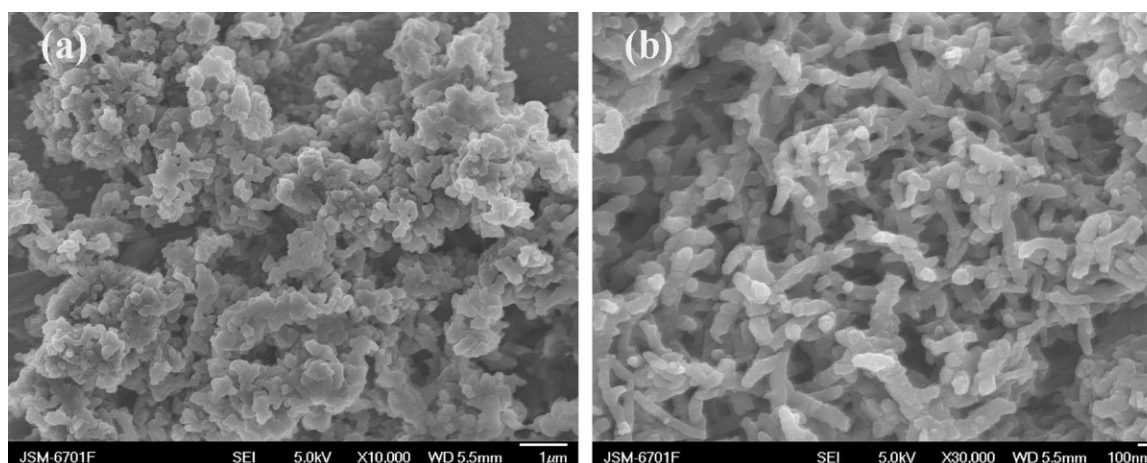


**Figure 3** SEM micrograph of GN/PANI composites: (a) lower magnification and (b) higher magnification.



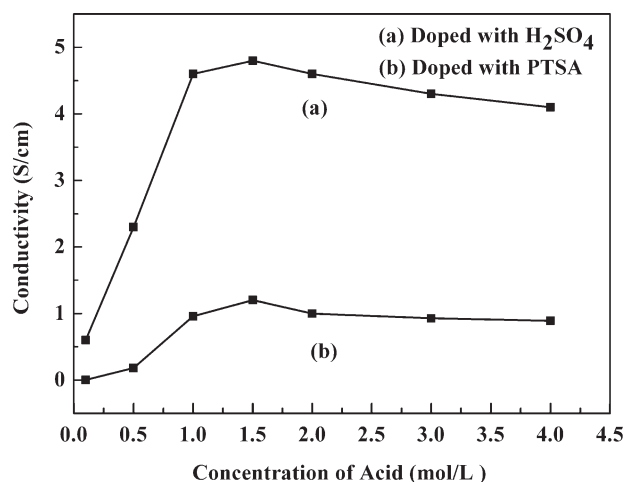


**Figure 4** Electrical conductivity of PANI versus acid: (a) H<sub>2</sub>SO<sub>4</sub> and (b) TSA and concentration.

that GN dispersed in PANI matrix and the PANI also embedded the GN. It was clearly observed from Figure 3(b) that the PANI appeared as rods, and the rods with the diameter of 100 nm and the length of 500–1000 nm. Furthermore, GNs were distributed quite uniformly within the PANI matrix and no aggregates can be seen in the mixture. Because of this especial structure, the interfacial affinity of GN with the PANI increased and led to an ensured thermal stability and electrical contact that served as the electrically conductive bridge. The results show that ultrasonic can effectively restrain the agglomerate of the aniline, and then GN can come to uniformity nanorods composites.

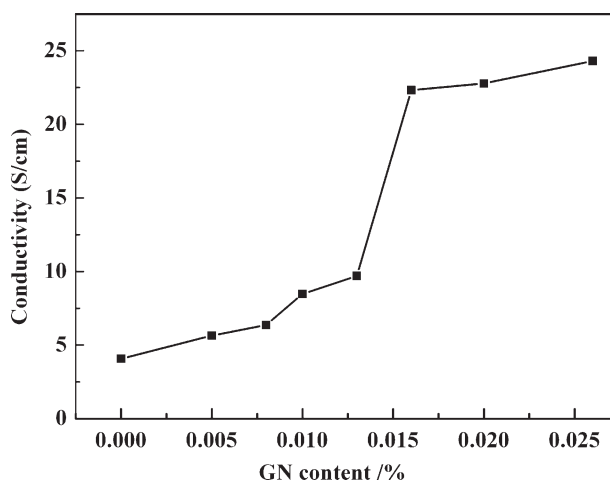
### Conductivity characteristics

Figure 4 shows the electric conductivity of PANI as a function of acid and concentration: An optimum acid concentration about 1.5 mol/L can be observed. The conductivity of the composites increase rapidly below this optimum and decreases with further increase in acid concentration. It can be noticed that the conductivity increases as the acid concentration increases, reaching a flat after which it decreases. With increasing acid concentration, the conductivity increases because of the increasing concentration of doped PANI. PANI is fully doped, and conductivity should show a maximum. The increase observed on the left side of the curve is attributed to the doping of the conducting polymer by acid, as the conductivity is related with the number of imine sites protonated. Conductivity increases as the protonated level of the imine sites approaches 50%. On the other hand, if the maximum doping reaches the high concentration of acid it leads to polymer degradation, with consequent decreasing in the conductivity. The

decrease of conductivity with increase of acid concentration may arise from the actual growth of dopant concentration, which has no electronic conduction. This behavior has been observed by Luiz et al.<sup>24</sup> and Yang and Ruckenstein.<sup>25</sup>

From Figure 4 we can clearly see that the conductivity of PANI doped with H<sub>2</sub>SO<sub>4</sub> always higher than PANI doped with TSA in the range we studied. It is expected that the conductivity of the doped PANI should change with different dopants, because the degree of doping is related to the density of charge carriers in the doped PANI. This may be attributed to the effect of dopant TSA-reduced interaction between doped PANI chains. Here, we only choose the representative inorganic and organic acid. The other doped acids will be researched in other work particularly.

The variation of electrical conductivity of GN/PANI nanorods composites versus the graphite content is shown in Figure 5. A feature of interest in this figure is that an abrupt conductivity transition occurs at a critical filler content, which can be designated as the percolation threshold. The composites containing GN exhibit a percolation threshold about 1.3 wt %; the conductivity of the GNs/PANI nanorods composites with GN content of only 1.3 wt % was found to be 22 S/cm, which was four times greater than that of neat PANI (about 4 S/cm). The electrical conductivity of the nanocomposites leveled off with the further increase of GN content. The electrical conductivity of GN was not deteriorated to a great degree compared with the original graphite flake. In this case, the nanocomposites prepared using GN as conducting fillers exhibited high electrical conductivity. The augmentation of the electrical conductivity can be ascribed to two facts: (1) we estimate that the nanoscale homogeneous dispersion of



**Figure 5** Electrical conductivity of GN/PANI composites versus GN content.

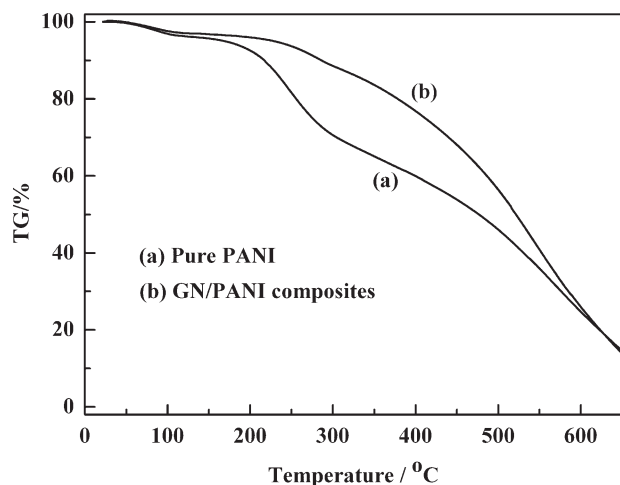


**Figure 6** Thermogravimetric curves of (a) PANI and (b) GN/PANI composites.

GNs in the polymer matrix resulting from ultrasonic irradiation and the formation of the conducting network,<sup>10,11,26</sup> and (2) the interaction between the big  $\pi$ -conjugated structure of the GN and the quinoid ring of PANI. The GN within the PANI matrix served as the electrically conductive bridge, which can enhance the conductivity between the polymer chains, according to the SEM analysis and our earlier study.<sup>9–11</sup> The result and analysis were similar to that reported by other researchers.<sup>26</sup> Compared with Du et al.'s experiment,<sup>26</sup> the results were in the same magnitude, but the reaction time was much shorter and the temperature was at 25°C, which can save more time and energy sources in large scale in the future.

All the earlier electrical conductivity datum were measured at ambient temperature (25°C) after the samples were dried in vacuum (80°C). So, the composites can be applied below the temperature (80°C), and it can meet the common use. We will research the conductivity characteristic and mechanism at higher temperatures in another article in detail.

### Thermogravimetric analysis

Figure 6 shows the TG curves of pure PANI and GN/PANI composites. It can be seen that the weight loss curve of nanocomposites appeared above that of pure PANI, indicating the enhanced thermal stability for the nanocomposites. The TG curves indicated that the onset decomposition temperature of GN/PANI nanorods composites was 250°C. It was higher than the decomposition temperatures of pure PANI, which was 210°C. It was because that there were strong interaction between large numbers of surface atoms of GNs and PANI molecule chains. And the

GN trammled the movement of the PANI molecule chains. It put the thermal decomposition of the composites at a disadvantage. Consequently, the needed energy of thermal decomposition increased, namely the thermal stability of composites increased. This increase in the thermal stability may result from the thermal barrier effect of the GN layers structure and from the interactions between PANI and NanoGs. Accordingly, the GN layers have a shielding effect and slow down the decomposition rate of the nanocomposite.

### CONCLUSIONS

The GN/PANI nanorods composites were fabricated via ultrasonic polymerization of aniline monomer in the presence of GN, which was used as electric filling. The nanoscale dispersion of GNs within the PANI matrix was evidenced by SEM examinations. From FTIR spectra analysis, it was reasonably concluded that there was strong interaction between PANI and GNs. An optimum doped concentration about 1.5 mol/L can be observed, and conductivity of PANI doped with H<sub>2</sub>SO<sub>4</sub> was always higher than PANI doped with TSA. The thermal stability of PANI exhibited a beneficial effect because of the introduction of GN. Electrical conductivity measurements indicated that the conductivity of final GN/PANI composites increased when compared with pure PANI because of the introduction of GN.

### References

- Genies, E. M.; Boyle, A.; Lapkowski, M.; Isintaus, C. *Synth Met* 1990, 36, 139.
- MacDiarmid, A. G.; Epstein, A. J. *J Chem Soc Faraday Trans* 1989, 5, 1.
- Wu, Q.; Xue, Z.; Qi, Z.; Wang, F. *Polymer* 2000, 41, 2029.
- Mehrotra, V.; Giannelis, E. P. *Solid-State Commun* 1991, 77, 155.
- Liu, P.; Gong, K. *Carbon* 1999, 37, 706.
- Xiao, P.; Xiao, M.; Liu, P. G.; Gong, K. *Carbon* 2000, 38, 626.
- Zheng, W. G.; Wong, S. C.; Sue, H. J. *Polymer* 2002, 43, 6767.
- Zheng, J. H.; Wu, J. S.; Wang, W. P.; Pan, C. Y. *Carbon* 2004, 42, 2839.
- Mo, Z. L.; Sun, Y. X.; Chen, H.; Zhang, P.; Zuo, D. D.; Liu, Y. Z. *Polymer* 2005, 46, 12670.
- Mo, Z. L.; Zuo, D. D.; Chen, H.; Sun, Y. X.; Zhang, P. *Eur Polym J* 2007, 43, 300.
- Mo, Z. L.; Zuo, D. D.; Chen, H.; Sun, Y. X.; Zhang, P. *Chin J Inorg Chem* 2007, 23, 265.
- Chen, G. H.; Wu, C. L.; Weng, W. G.; Wu, D. J.; Yan, W. L. *Polymer* 2003, 44, 1781.
- Weng, W. G.; Chen, G. H.; Wu, D. J. *Polymer* 2005, 46, 6250.
- Chen, G. H.; Lu, J. R.; Wu, D. J. *J Mater Sci* 2005, 40, 5041.
- Chen, G. H.; Weng, W. G.; Wu, D. J.; Wu, C. L. *Eur Polym J* 2003, 39, 2329.
- Du, X. S.; Xiao, M.; Meng, Y. Z. *J Polym Sci Part B: Polym Phys* 2004, 42, 1972.

17. Du, X. S.; Xiao, M.; Meng, Y. Z.; Hay, A. S. *Polymer* 2004, 45, 6713.
18. Tursun, A.; Ruxangul, J.; Ismayil, N. *J Appl Polym Sci* 2007, 105, 576.
19. Ding, Y. j.; Tursun, A.; An, S. Y.; Ismayil, N. *J Appl Polym Sci* 2008, 107, 3864.
20. Habsuda, J.; Simon, G. P.; Cheng, Y. B.; Hewitt, D. G.; Diggins, D. R.; Toh, H. *Polymer* 2002, 44, 4627.
21. Wang, J. J.; Zhu, M. Y.; Outlaw-Ron, A.; Zhao, X. *Carbon* 2004, 42, 2867.
22. Chen, G. H.; Weng, W. G.; Wu, D. J.; Wu, C. L.; Lu, J. R.; Wang, P. P. *Carbon* 2004, 42, 753.
23. Fukuda, K.; Kikuya, K.; Isono, K.; Yoshio, M. *J Power Sources* 1997, 69, 165.
24. Luiz, F. M.; Giovana, A. L.; Simone, C. L. *Eur Polym J* 2006, 42, 3108.
25. Yang, S.; Ruckenstein, E. *Synth Met* 1993, 59, 1.
26. Du, X. S.; Xiao, M.; Meng, Y. Z. *Eur Polym J* 2004, 40, 1489.